

Understanding the release behavior of folic acid through liquid-crystalline folate nanoparticles: Process optimization through Response-Surface methodology and Mathematical modeling using Noyes-Whitney approach

Rahul Misra¹ and Sanat Mohanty*¹

¹*Advance Materials & Nanoscience Laboratory, Department of Chemical Engineering, Indian Institute of Technology-Delhi, Hauz Khas, New Delhi-110016, India*

* *Corresponding author*

ABSTRACT

In our previous studies we have shown the potential of folate nano-carriers in releasing the encapsulated chemotherapeutic drugs at controlled rates. Also, we have seen that the release rates of encapsulated drugs and the carrier (folic acid) are comparable and can be regulated by different design parameters like particle size and cross-linking. To achieve different release rates, the design parameters have to be optimized. Therefore, we need to understand how different factors simultaneously affect the release behavior of folic acid (and/or drugs). With the use of Response-surface methodology approach, this article understands the combined effect of different factors affecting the release behavior and optimizes different parameters to obtain desired folic acid release. Also, with the help of drug dissolution model, the present article understands the mechanism of release behavior and the role of design parameters in controlling the release rates.

KEY WORDS: FOLATE, LIQUID-CRYSTALLINE, CONTROL RELEASE, RESPONSE SURFACE METHODOLOGY, PROCESS OPTIMIZATION, NOYES-WHITNEY

INTRODUCTION

Different drug delivery models are used routinely to help optimizing the design of novel dosage forms. Considering the desired type of administration, drug dose to

be incorporated and targeted drug release profile, mathematical predictions can provide good estimates of the required composition, geometry, dimensions and preparation procedure of the respective dosage forms. The use of mathematical modeling in drug delivery will help in

ARTICLE INFORMATION:

Received 21st November, 2015

Accepted 5th December, 2015

BBRC Print ISSN: 0974-6455

Online ISSN: 2321-4007 NAAS Journal Score : 3.48

© A Society of Science and Nature Publication, 2015. All rights reserved.

Online Contents Available at: <http://www.bbrc.in/>

saving development time and to reduce costs. Also, the number of required experimental studies to develop a new and/or optimize an existing drug product can significantly be reduced (Siepmann 2013, Siepmann 2001).

In addition, mathematical modeling is also used for the quantitative analysis of the physical, chemical and potentially biological phenomena involved in the control of drug release. The underlying drug release mechanisms can be elucidated. This understanding will help in efficient improvement of the safety of new pharmaco-treatments, especially for highly potent drugs with narrow therapeutic windows. Furthermore, potential challenges encountered during production (trouble-shooting) can be much more efficiently addressed (Arifin 2006, Ashlee 2013).

Previous studies report several mathematical theories (Lin 2006, Narsimhan 2001). Most of them lack broad range accuracy across drugs or delivery systems but are reasonably accurate for specific drugs in certain dose range. These include *empirical/semi-empirical* as well as *mechanistic models*. Some computational and stochastic models were also developed for drug delivery systems with the aim of understanding and modeling the complexity in biological phenomenon, which may help in designing new drugs as well as in predicting the drug metabolism inside the human body (Gadgil 2008, Costo 2001).

These types of models allow for the determination of system-specific parameters that can offer deeper insight into the underlying drug release mechanisms; for instance, the relative importance of several processes that are involved (e.g., drug diffusion and polymer swelling) can be estimated. There are different mechanisms of drug release, for example, drug dissolution, diffusion, swelling of a matrix, degradation of matrix, etc (Lemaire 2003, Mallapragada 1998, Narsimhan 1997, Vaidyanathan 2014).

Generally, on contact with aqueous body fluids, the drug from the nanoparticles is released in a controlled manner depending upon the mechanism. This drug dissolves in the fluid and reaches to target cells by crossing different physiological and chemical barriers. The present study evaluates the only model release mechanism and not the transport across different barriers inside the body.

DRUG DISSOLUTION, DIFFUSION AND DRUG RELEASE: NOYES –WHITNEY APPROACH

Out of numerous processes in human body, diffusional mass transport phenomenon is the most fundamental and was reported first by Fick in 1855. Briefly, spontaneous transport of substances dissolved in gases, liquids or solids, from regions of higher concentration to regions of lower concentration is referred as diffusion. The components which will solubilise will diffuse with the aqueous phase. Thus, if a drug exhibits very low solubility in water and/or if its mass transfer rate at the

site of administration is very low, minor amounts of drug will be available for diffusion. This might result in insufficient drug concentrations at the site of action (Siepmann 2013, Siepmann 2001).

A better understanding of the physico-chemical reasons for poor aqueous solubility and/or very low mass transfer rates can be very helpful in designing. Thus, quantitative and mechanistically realistic mathematical modeling of the process of drug dissolution can be highly beneficial. Potential mass transport phenomena to be taken into account include the wetting of the particle's surface with water, possible disintegration of particles or diffusion through the carrier matrix, the solvation of individualized drug molecules/ions, the diffusion of drug molecules/ions through the liquid, unstirred boundary layer, which surrounds the drug particles, and convection within the surrounding bulk fluid. Several drug dissolution models have been reported in the literature for the control drug release mechanism (Siepmann 2013, Siepmann 2001). Noyes-Whitney model is one of them.

RESPONSE SURFACE METHODOLOGY

Response Surface Methodology (RSM) is a collection of mathematical and statistical techniques for empirical model building. The objective behind using RSM is to optimize a response (output variable) which is influenced by several independent variables (input variables) by using design of experiments. An experiment is referred as series of tests, called runs. In these runs, changes are made in the input variables to identify the reasons for changes in the output response. (Box and Wilson, 1951). Response surface methodology is a widely practiced approach in the optimization of drug delivery processes. It is a useful tool in the development and optimization of controlled release of drugs through nanoparticles (Ko 2003, Kumari 2009, Bezarra 2008). Different steps involved in response surface methodology include experimental design, regression analysis, generation of polynomial equations, and mapping of the response over the experimental domain to determine the optimum formulation(s). The technique reduces the number of experiments required to be conducted, therefore proving to be time and cost-effective than the conventional methods of formulating dosage forms. In the present investigation, the effect of factors (pH of release medium, size of nanoparticle, release time) that can influence the drug release and loading was investigated.

OPTIMIZATION OF FOLIC ACID RELEASE THROUGH RSM

There are different types of response-surface models for example, full-factorial design, Central-composite design

Table 1: Experimental range and levels of the independent variables					
Independent variable	Range and levels (coded)				
	- α	-1	0	+1	+ α
pH (A)	2	3.62	6	8.38	10
Release time, hours (B)	2	52.27	126	199.73	250
Size, nm (C)	30	125.27	265	404.73	500

(CCD), Box-Behnken design and Taguchi model. In the present study, percentage release of folic acid was studied using CCD. It is a good approximation of second-order model as it reduces the number of experiments. It is expressed according to the equation (1):

$$Y = \beta_0 + \sum_{i=1}^k \beta_i x_i + \sum_{i=1}^k \beta_{ii} x_i^2 + \sum_{i=1}^{k-1} \sum_{j=i+1}^k \beta_{ij} x_i x_j + \varepsilon \quad (1)$$

In equation (1), Y is response (dependent variable); β_0 is constant coefficient; β_i , β_{ii} and β_{ij} are coefficients for the linear, quadratic and interaction effect; x_i , x_j are factors (independent variables) and ε represents the error. Three factors were studied and their low and high levels are given in Table 1. The second-order model includes all the terms in the first-order model, plus all quadratic terms like $\beta_{ii} x_i^2$ and all cross product terms like $\beta_{ij} x_i x_j$. The second-order model is flexible, because it can take a variety of functional forms and approximates the response surface locally. Therefore, this model is usually a good estimation of the true response surface (Chowdhury 2012).

We have previously reported the formation of folate self assembly and a process to develop nanoparticles from self-assembled liquid-crystalline folates. Moreover, a method to control the size of these nanoparticles was also reported. An extensive study was carried out to understand the disintegration of particles and recognizing the parameters to control the release rates of encapsulated drugs from these particles (Misra 2014). It was observed that the release behavior of folic acid resembles the release behavior of encapsulate drugs. For desired release rates and efficient designing, there is a need to optimize the design parameters for nanoparticles developed.

It is important to understand the combined effects of different parameters and their role in folic acid release. Modeling and optimization of folic acid release behavior will give a clear insight of correlations between design parameters, particle break-up and drug release. Our aim in the present study is to understand the release behavior and to improve mechanistic understanding of release from the carrier, so to achieve better design of the folate carrier.

MATERIALS AND METHODS

PREPARATION OF LIQUID-CRYSTALLINE FOLATE NANOPARTICLES

An extensive study in the design of folate nanoparticles, thermodynamics of particle formation and characterization has been described elsewhere (Misra 2014). In brief, folate nanoparticles can be developed from liquid-crystalline folate solution by mixing it with HPMC (Hydroxy Propyl Methyl Cellulose) polymer and their size can be controlled by varying the relative concentrations of both components in the solution. Folic acid by itself does not dissolve in water; however in the presence of NaOH it forms the liquid crystalline solutions. It has been reported in the past that folic acid molecules get completely ionized by NaOH and can be dissolved in water easily. Liquid-crystalline behavior is observed between the pH values 6.5 and 7.5 (Misra 2014). HPMC is a water soluble cellulosic biocompatible polymer used in the food industries as additives, emulsifier, and thickening and suspending agents.

CONTROL RELEASE STUDIES OF FOLIC ACID

We have studied the release behavior of folic acid and encapsulated drugs in detail and reported the design and process parameters responsible for regulating the release rates of folic acid and drugs. Also, it was observed that the release rates of folic acid and drugs were same (Misra 2014, Misra 2014). Therefore, in the present case we are considering only the release behavior of folic acid for optimization and modeling study.

DESIGN OF EXPERIMENTS: CENTRAL COMPOSITE DESIGN (CCD)

The central composite design, CCD, is used to build a second order experimental model. CCD is composed of a factorial design, a set of central points, and axial points equidistant to the center point. The factorial design component of CCD is of the class 2^k factorial where k represents the number of relevant factors or variables. Each of the variables is taken at two levels meaning that each variable has a low and high numeric value. A coded numeric value of -1 and +1 is assigned to represent the variable's low and high values. The geometric representation of a factorial is a cube in which each corner represents an interaction of the factors. In this perspective, 8 interactions are to be evaluated when 3 processing variables are selected to determine their significance in the final response (Ko 2003, Kumari 2009).

The axial component of CCD refers to the points that are equidistant from the center of the cube formed for the factorial design. A spherical design is obtained since there

is an equal variance from the center to all the points in the sphere. In consequence, there is a positive axial value (+ α) and a negative axial value (- α). The axial points add two more levels in each variable. The value of α is calculated from the equation $\alpha = (ni)^{1/4}$ where, ni represent the number of interactions obtained from the factorial design. Thus, for 8 interactions $\alpha = 1.682$. The central point component in the CCD is the average of the high and low values determined in the factorial design. The central point or zero point may be defined as the region where the optimal conditions are supposedly met. The addition of the central point in the design increases the level in one unit to a total of 5 levels for each variable (Myers 1976, Gilmour 2006).

In the present study, a 2^3 full factorial central composite experimental design was used to optimize the release of folic acid. Twenty experiments were conducted in duplicate according to the scheme mentioned in Table 2. Design Expert ver. 9 (Stat Ease, USA) software was used for regression and graphical analysis of the data obtained. The optimum values of the selected variables were obtained by solving the regression equation and by analyzing the response surface contour plots. The variability in dependent variables was explained by the multiple coefficient of determination, R^2 .

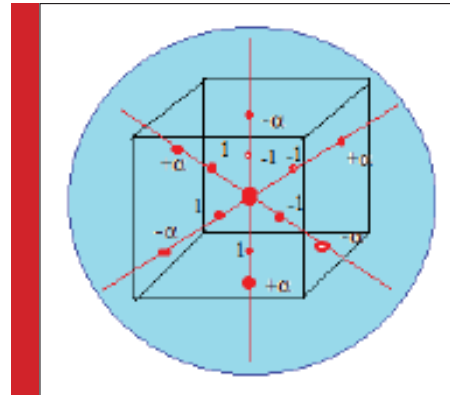


FIGURE 1: Layout of the Central Composite Design (CDD) for 3 variables at 5 levels.

The model equation was used to predict the optimum value and subsequently to elucidate the interaction between the factors within the specified range. The optimization of folic acid release was carried out by three independent process variables including pH of the release medium, size of the nanoparticles and release

Table 2: Central composite design for three independent variables used in this study along with the observed response at 3 coded levels.

Run no.	Coded values			Real values			Response 1: R1
	Factor A: pH	Factor B: Release time hours	Factor C: Size (nm)	Factor A: pH	Factor B: Release time hours	Factor C: Size (nm)	Percent release of folic acid %
1	-1	-1	-1	3.62	52.27	125.27	6
2	+1	-1	-1	8.38	52.27	125.27	14
3	-1	+1	-1	3.62	199.73	125.27	4
4	+1	+1	-1	8.38	199.73	125.27	20
5	-1	-1	+1	3.62	52.27	404.73	8
6	+1	-1	+1	8.38	52.27	404.73	20
7	-1	+1	+1	3.62	199.73	404.73	13
8	+1	+1	+1	8.38	199.73	404.73	60
9	- α	0	0	2	126	265	1
10	+ α	0	0	10	126	265	24
11	0	- α	0	6	2	265	4
12	0	+ α	0	6	250	265	28
13	0	0	- α	6	126	30	7
14	0	0	+ α	6	126	500	50
15	0	0	0	6	126	265	32
16	0	0	0	6	126	265	32
17	0	0	0	6	126	265	32
18	0	0	0	6	126	265	32
19	0	0	0	6	126	265	32
20	0	0	0	6	126	265	32

time. The ranges and levels of variables investigated in the study are given in Table 1. The percent release of folic acid was taken as response of the system. Table 2 represents the central composite design of experiments with total of 20 experiments at 3 coded levels.

RESPONSE SURFACE ESTIMATION FOR MAXIMUM RELEASE OF FOLIC ACID

The condition of each experiment performed as per this algorithm and the release data are given in Table 2. An empirical relationship between the response and the independent variables has been expressed by the following quadratic model.

Final Equation in Terms of Coded Factors:

$$\% \text{ release of folic acid (R1)} = 30.8 + 8.91A + 9.55B + 9.47C + 4.88AB + 4.38 AC + 4.63BC - 7.28 A^2 - 2.15B^2 - 1.62C^2$$

The statistical significance of the model equation was evaluated by the *F*-test ANOVA. Positive sign in front of these three terms represents synergistic effect, while negative sign represents antagonistic effect. The coefficients with one factor of pH, release time and size represent the effect of that particular factor on the percent release of folic acid. The coefficients with two factors and others with second order terms show the interaction between the two factors and quadratic effect, respectively. The accuracy of the model developed can be understood by the value of R^2 , adjusted R^2 and standard deviation. R^2 indicates the ratio between sum of the squares (SSR) with total sum of the square (SST) and it describes up to what extent perfectly the model estimated experimental data points (Bezerra 2008, Ko 2003).

MODELING OF FOLIC ACID RELEASE USING NOYES-WHITNEY MODEL

This model is based on drug dissolution through a boundary layer and the diffusional mass transport step through the liquid, with transport through the boundary layer being the rate limiting process. According to this model, "the rate at which a solid substance dissolves in its own solution is proportional to the difference between the concentration of that solution and the concentration of the saturated solution". Based on observation of two quite different materials dissolving in distilled water, Noyes and Whitney deduced the general law (Siepmann 2001):

$$\frac{dc}{dt} = K(C_s - C) \quad (1)$$

Where dC/dt is the dissolution rate; K is a mass-transfer constant; C_s denotes the solubility of the substance, and C is the concentration of dissolved substance in bulk. Noyes and Whitney obtained values for the solubility C_s and the concentration C for several values of t . With

these values and equation (1), values for the constant K were determined for benzoic acid and lead chloride dissolving in distilled water. For their system, K remains constant for a particular binary system of a solute A and solvent B (Siepmann 2001).

Model Description And Assumptions

In the present study, it has been assumed that the particles are surrounded by a boundary layer and the movement of released folic acid molecules from the particle into the bulk medium is a two stage process 1) Dissolution of released folic acid next to the surface of the particle; 2) Movement of folic acid molecules from boundary layer to bulk release medium. A schematic representation of these steps has been shown in figure 2. The folic acid (and the drug molecules) released dissolves next to the particle which represents the surface concentration (C_s) of release folic acid (and drug). These molecules will move into the bulk release medium overcoming the boundary layer resistance due to the mass transfer. With dissolution, there is a reduction in particle size.

Most of the models including Noyes-Whitney equation assume that the concentration of a mass on the surface, C_s is constant over release time (figure 2). In this study, C_s has not been assumed to be constant, as the concentration at the surface (C_s) is not at equilibrium with the concentration in bulk medium (C). The value of C_s is a result of the rate of dissolution and the rate of mass-transfer across boundary layer. For low to moderate dissolving drugs, the mass-transfer across boundary layer is also significant. Hence, C_s cannot be a constant over release time. The underlying assumptions of the developed mathematical model are: (i) The released folic acid dissolves next to the particle (C_s). (ii) The solid particles have a constant size at initial time. The particle size reduces as the drug dissolution advances until complete dissolution of the particles. (iii) The particles are assumed to be spherical for simplicity. This is a good assumption validated through TEM images. (iv) Due to

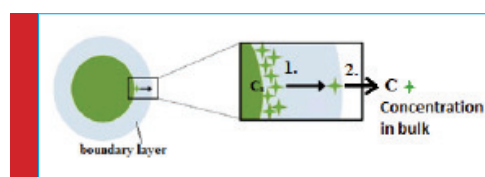


FIGURE 2: Schematic representation of folic acid release from surface to bulk medium across boundary layer as a two step process. 1) Dissolution of released folic surface next to the particle surface, 2) Drug dissolution from boundary layer to bulk medium. C_s denotes concentration at the surface, while C denotes the concentration in bulk fluid.

boundary layer mass transfer, released folic acid moves to bulk liquid. (vii) Mass transfer coefficient (K) changes with different conditions. (viii) C_s is not constant, but changing with different conditions.

A model for the present study was developed based on Noyes-Whitney equation. Integrating and re-arranging the equation (1) with appropriate assumptions gives:

$$\ln \frac{(C_s - C_{tf})}{(C_s - C_{t_0})} = -Kt \quad (2)$$

Where C_{tf} and C_{t_0} are the concentration of substance at final release time ($t = t_f$) and initial release time ($t = t_0$). In the model equation, C_{tf} and C_{t_0} were the experimentally recorded values at final time (t_f) and initial time (t_0) respectively.

For in-vitro release studies, 0.04 gms of lyophilized folate nanoparticles are suspended in 10 ml of release medium in vials for a particular time (t_p). During static mode studies, these vials are kept undisturbed while for shaking mode studies, these vials are kept under mild shaking (100rpm) through orbital shaker. After time (t_p), vials are centrifuged at 2000 rpm and 9 ml of supernatant was collected in separate vial while vials containing nanoparticles are again replenished with fresh medium for further release study. The process is repeated after every periodic interval. Thus, release from a single sample is studied over n periods, each of time t_f . The released concentration was recorded in the harvested supernatant after each of the n periods.

It has been assumed that C_s is constant during each of the n periods. However, it changes from one period to the next. This is a reasonable approximation if the periods are chosen appropriately. The experimental values of C_{tf} and C_{t_0} fitted to the model equation by plotting a graph between $\ln(C_s - C_{tf}/C_s - C_{t_0})$ and release time t . The slope of this plot (figure 3) represents the change in mass-transfer coefficient, K ; while, the value of surface concentration at different time was calculated from the equation. On the basis of R^2 values (regression coefficient), we can say that the experimental data fits to the model equation well. However, at initial time intervals between 0-200 hours, the experimental data does not fit well to the model equation. This can be due to higher release rate observed during initial period of 8-24 hours.

RESULTS & DISCUSSION

PROCESS OPTIMIZATION THROUGH RSM: STATISTICAL ANALYSIS OF THE RESPONSE-SURFACE MODEL

The competence and significance of the model in the present study was justified by analysis of variance (ANOVA). The

Table 3: Statistical analysis of data through regression model.

Regression analysis for Response Surface Quadratic Model				
Model term	Coefficient estimate	Standard error	F-value	P-value
A	8.91	0.74	21.41	<0.0001
B	9.55	0.74	24.58	<0.0001
C	9.47	0.74	24.18	<0.0001
AB	4.88	0.97		0.0006
AC	4.38	0.97	3.02	0.0814
BC	4.63	0.97	3.38	0.1127
A ²	-7.28	0.72		<0.0001
B ²	-2.15	0.72	1.32	<0.0001
C ²	-1.62	0.72		<0.0001

statistical analysis results of response surface quadratic model in the form of analysis of variance (ANOVA) are shown in Table 3 and 4. The significance of each coefficient was determined by F -values and P - values.

Table 3 shows that the coefficients for the main and square effects were highly significant ($P < 0.0001$) in comparison with interaction effects. This shows that the model terms are significant. In this case, A, B, C and A², B², C² are significant model terms. The model F -value (110.69) in table 4 show a low probability value ($P < 0.0001$) which demonstrates a high significance for the quadratic model. The goodness of fit of the model was also checked by the multiple correlation coefficient (R^2). Table 4 show the value of the multiple correlation coefficient as 0.9764, which revealed that this regression is statistically significant and only 1.36% of the total variations is not explained by the model. The value of predicted multiple correlation coefficient (pred. $R^2 = 0.9420$) is in reasonable agreement with the value of the adjusted

Table 4: Statistical analysis of data through ANOVA.

ANOVA for Response Surface Quadratic Model Analysis of variance table [Partial sum of squares - Type III]					
Source	Sum of Squares	Degree of freedom (df)	Mean Square (MS)	F-Value	p-value Prob >F
Model	5225.19	9	541.5	110.69	<0.0001
Residual	75.28	10	7.53		
Lack of fit	75.28	5	15.06	2.73	0.5271
Pure error	0.000	5	0.000		
Total	5375.75	19			

$R^2 = 0.9764$; Adjusted $R^2 = 0.9631$; Predicted $R^2 = 0.9420$.

multiple correlation coefficient (adj. $R^2 = 0.9631$). The non-significant value of lack of fit (0.527) showed that the quadratic model was valid for the present study.

EFFECT OF INDEPENDENT PARAMETERS ON DEPENDENT PARAMETERS

Response surface graphs were generated using the above quadratic model equation, which represent the simultaneous effect of any two variables on response param-

eters by taking one variable at a constant level. Coefficients with one factor in equation are attributed to the effect of that particular factor, while the coefficients with more than one factor are attributed to the interaction between those factors. A positive sign of the terms in equation indicates a positive effect, while a negative sign indicates a negative effect of the independent factors (Chowdhury 2012). A positive effect leads to an increase in response values while a negative effect leads to decrease in response values.

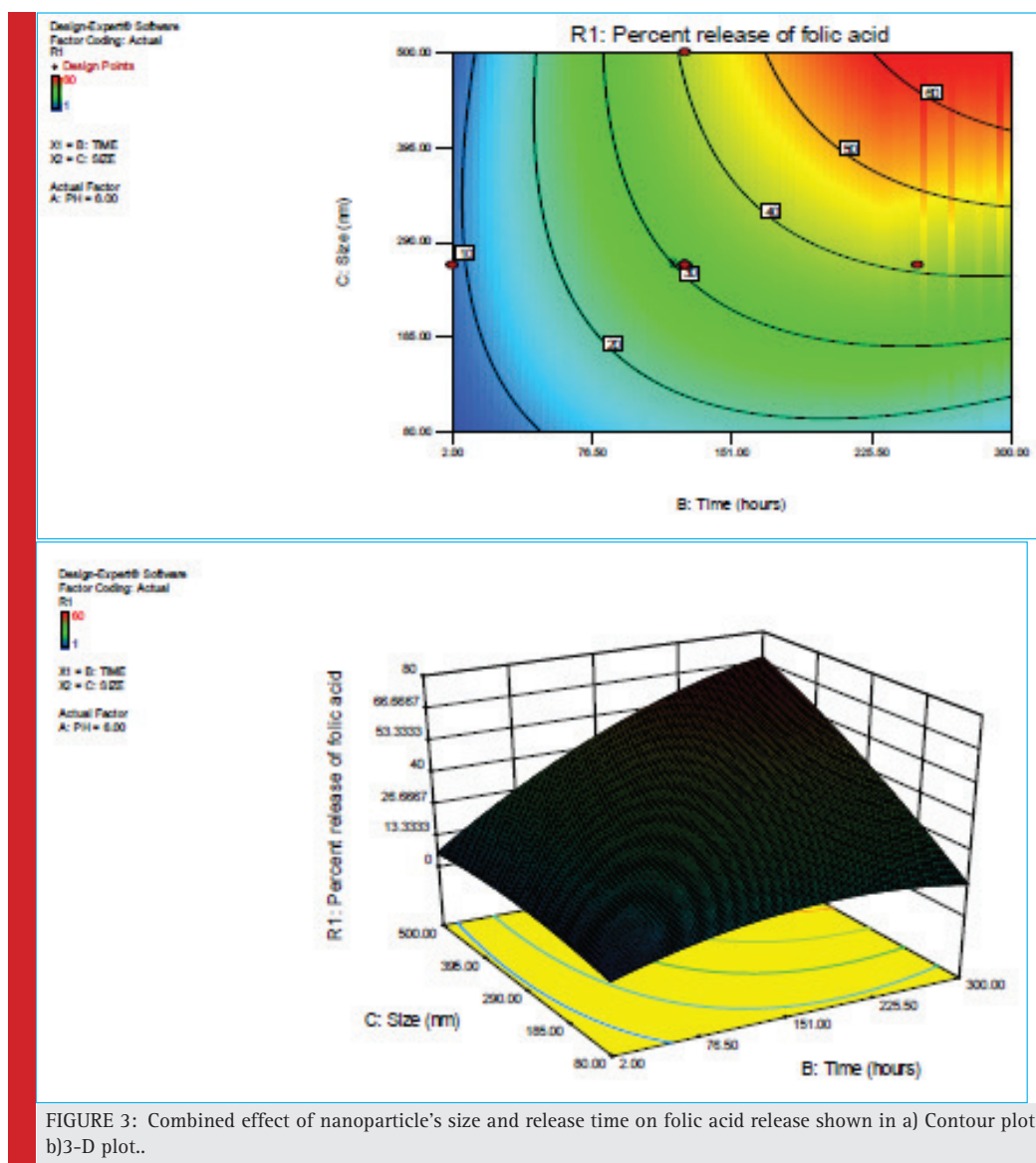


FIGURE 3: Combined effect of nanoparticle's size and release time on folic acid release shown in a) Contour plot b)3-D plot..

Effect of nanoparticle's size and release time on folic acid release

The contour plot (figure 3a) illustrates the interaction effects of the independent variables (size of nanoparticles and release time) on the response process. The size of nanoparticles and release time shows a remarkable effect on the release rates of folic acid.

With release time, the release of folic acid increases. Moreover, according to the contour plot in figure 3a,

percent release of folic acid increased as the nanoparticle size increased. The primary factor explaining this characteristic is that decreasing nanoparticle size increases the surface area which favors more effective cross-linking. Nanoparticles with highly cross-linked folate assembly is difficult to disrupt, therefore release of folic acid from smaller particles is slow. Similar trends were observed while studying the effect of single parameter on release of folic acid and drug.

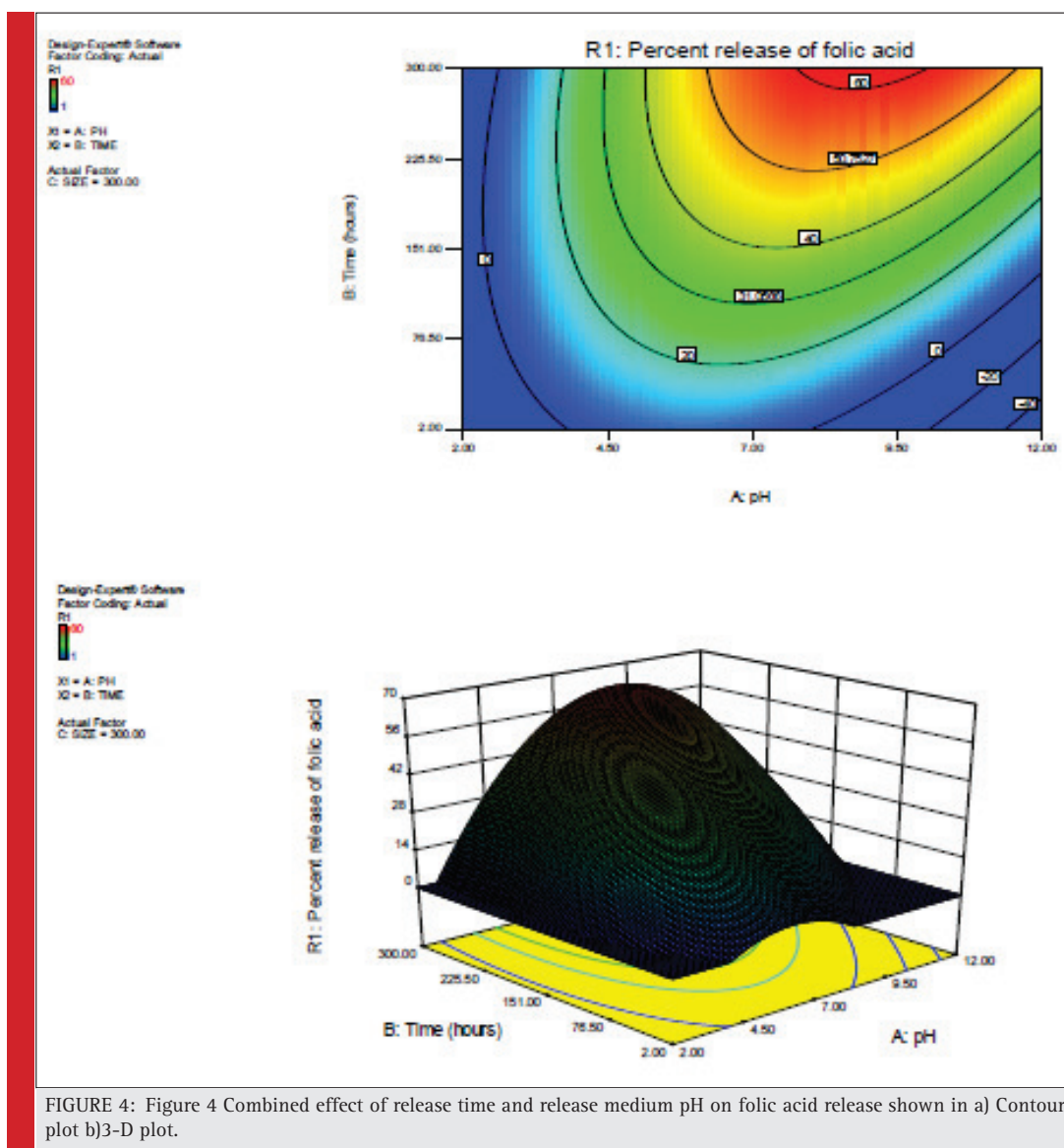


FIGURE 4: Figure 4 Combined effect of release time and release medium pH on folic acid release shown in a) Contour plot b)3-D plot.

Effect of release medium pH and release time on folic acid release

The effect of different levels of pH and release time on folic acid release can be predicted from the contour plot as shown in figure 4. It is evident from contour plot that both the independent variables had a strong influence on the release rates.

The release of folic acid is increasing with release time. Negligible release was observed in highly acidic

(pH 2-3) and basic pH (pH 10-12) regions. However, there is a significant increase in the release observed above pH 4, with maximum release recorded between pH 7-8. From the contour plot, a maximal percent release of 60% was observed with 300nm particle in 280 hours at pH 8. As described before, solution pH affects the chemistry of the release process; therefore the release process is strongly pH and release time dependent.

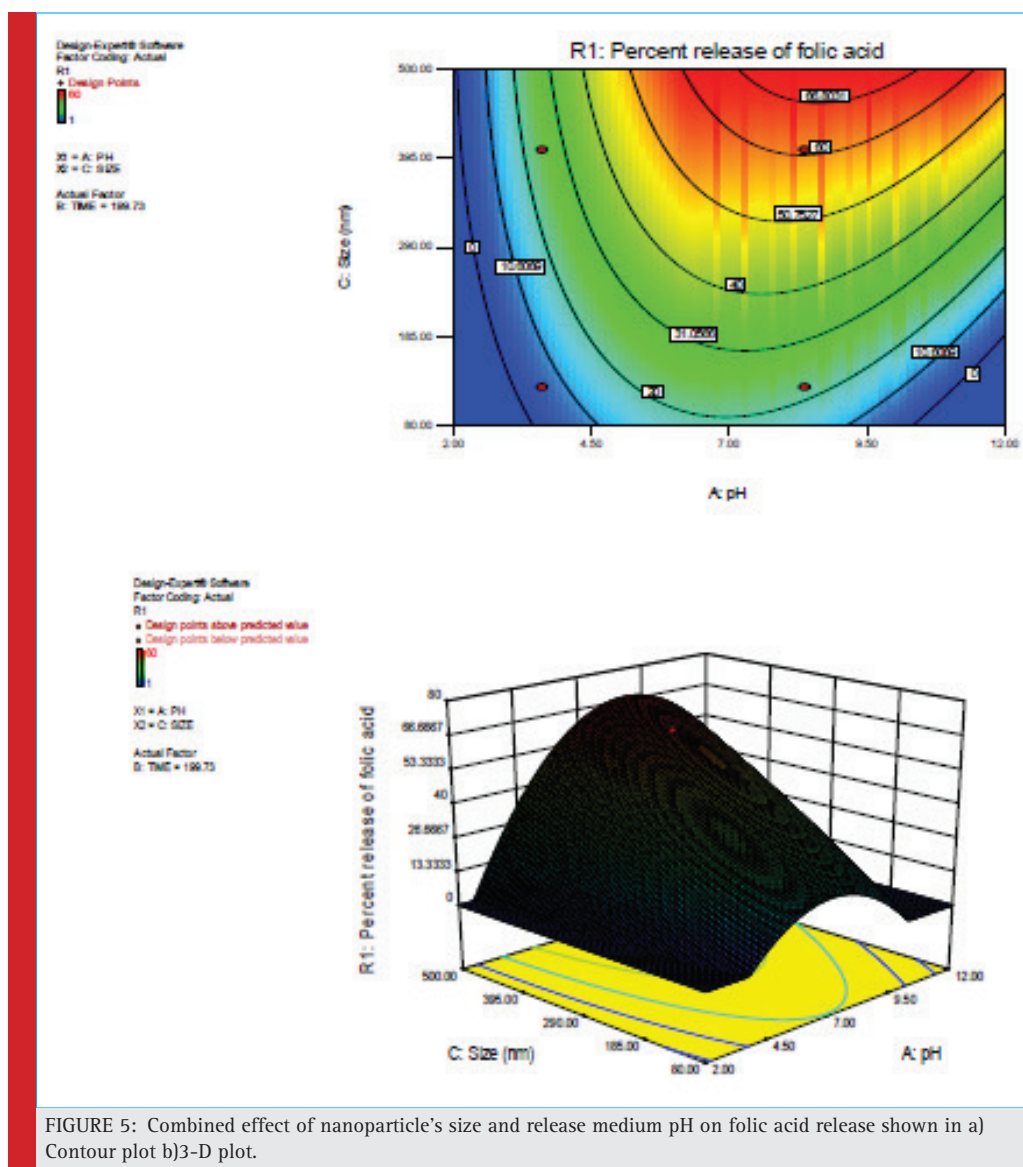


FIGURE 5: Combined effect of nanoparticle's size and release medium pH on folic acid release shown in a) Contour plot b)3-D plot.

Effect of release medium pH and nanoparticle's size on folic acid release

The combined effect of release medium pH and size of the nanoparticles on folic acid release is shown in the contour and 3D plot of figure 5. It is observed that percentage release of folic acid increased with increasing the size of the nanoparticles.

In addition, it was observed that there is an increase in release with increasing pH in the range of 2-8. Subsequently, increase in pH beyond 8, causes a decrease in release. This means that higher values of folic acid release can be obtained by increase in size of nanoparticles and a release medium pH at approximately 8. From this contour plot, a maximal percent release of 66.8% was achieved with 460nm particle and release medium pH 8 in 200 hours. Though particles of size higher than 460nm will give high release rates but in respect to drug delivery applications, size range of 30-500nm is desirable. Therefore this range was selected to study the optimization of release from the particles of this range.

OPTIMIZATION USING THE DESIRABILITY FUNCTION

This model has shown the interactions of two independent variables and their combined effect on the response. Additionally, it is of interest to study the combined effect of all the three variables on the response, for which the numerical optimization of 3 parameter system was carried out.

When a system has multiple responses for given experimental factors, individual optimization of factors becomes difficult, because what is optimal for one response may not be optimal for other responses. Desirability function approach is powerful tool for solving the multiple response optimization problems; where all the objectives are attain a definite goal simultaneously. The basic idea of this approach is to convert a multiple response optimization problem into a single response optimization problem with the objective function of overall desirability. Then the overall desirability function is optimized. The general approach is to first convert each response y_i , into an individual desirability function d_i , that may vary over the range $0 \leq d_i \leq 1$, where if the response y_i meets the goal or target value, then $d_i = 1$, and if the response falls beyond the acceptable limit, then $d_i = 0$. The next step is to select the parameter combination that will maximize overall desirability D (Chowdhury 2012, Myers 1976). The goals are combined into an overall desirability function. Desirability is an objective function that ranges from zero outside of the limits, to one at the goal. The program seeks

to maximize this function. The goal seeking begins at a random starting point and proceeds up the steepest slope to a maximum. There may be two or more maximums because of curvature in the response surfaces and their combination in the desirability function.

A multiple response method was applied for optimization of any combination of four goals, namely size of nanoparticles, pH, release time and percent release of folic acid. The numerical optimization found a point that maximizes the desirability function. A minimum level of nanoparticle's size (30 nm), minimum level of release time (2 hours), maximum percentage release (100%) and the level of release medium pH within the range of 6.0 to 8.0 were set for maximum desirability. The system was optimized to achieve maximum release possible within these above mentioned constraints. These constraints were selected as maximum release was observed within the pH range 7-8. The desirable size range for nanoparticles is 30-500nm for drug delivery applications. Therefore we were interested in determining the optimized values of all the variables along with the release within these constraints. The major goal was to achieve the optimized values of maximum release at minimum release time with smallest size nanoparticle possible in the pH range of 6-8. Figure 6 shows a ramp desirability that was generated from 10 optimum points via numerical optimization. Table 5 describes how these ramps generated according to the desirability and set constraints. These ramps indicate the desirability range and constraints (Chowdhury 2012). These ramps show competing trends of all the variables during optimization of response.

By seeking from 10 starting points in the response surface changes, the best local maximum was found to be at pH 7.82, nanoparticles of size 216.8nm at release time of 182.54 hours, folic acid release of 36.43% was predicted with the desirability of 0.843. The obtained value of desirability (0.843) shows that the estimated function may represent the experimental model and desired conditions.

CONFIRMATION EXPERIMENTS

Figure 7 shows the relationship of experimental versus predicted data of two independent factors. On the basis of predicted and experimental R^2 values, we can say that there is a strong agreement between predicted and experimental data. Figure 10.6 shows that predicted response is closer to the experimental response obtained. To support the optimized data given by numerical modeling under optimized conditions, confirmatory experiments were conducted with the parameters as suggested by the model (pH 7.82, 217 nm particles cross-linked with zinc, release time 183 hours) and the percent removal was found to be 34%.

Table 5: Description of ramps showing desirability according to the constraints.			
Variables	Constraints	Desirability 0	Desirability 1
pH (6-8)	In range 6-8	below pH 6 and above pH 8	pH 6-8
Size of nanoparticles (30-500nm)	Minimize to 30nm	500nm	30nm
Release time (2-494) hours	Minimize to 2hours	494 hours	2 hours
Release 1-100%	Maximize to 100%	1%	100%

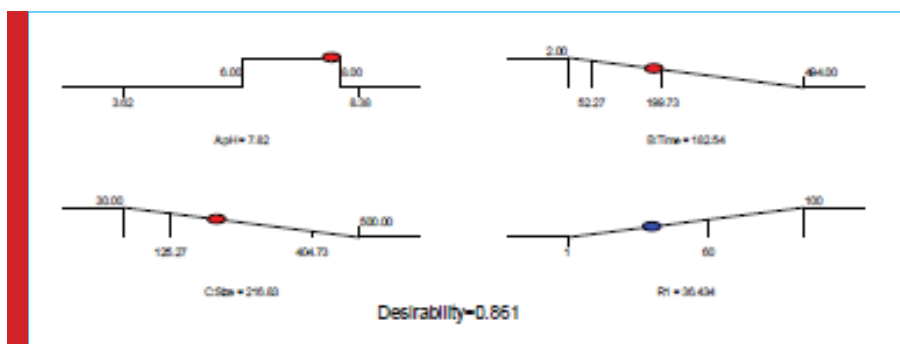


FIGURE 6: Desirability ramp for numerical optimization of four goals, namely pH of release medium (factor A), release time (factor B, hours), Size of the nanoparticles (factor C, nm) and Percent release of folic acid (Response RI, %).

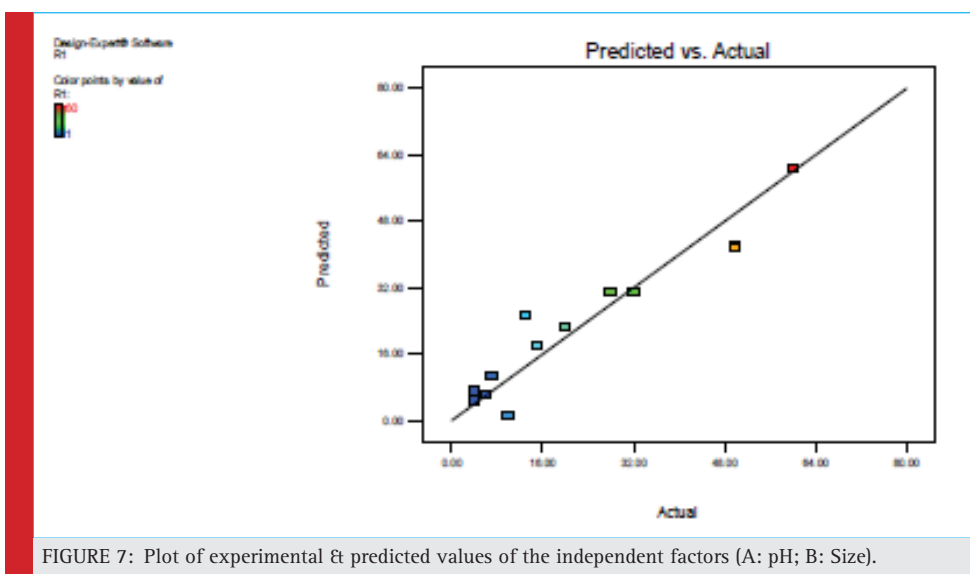


FIGURE 7: Plot of experimental & predicted values of the independent factors (A: pH; B: Size).

MODELING OF FOLIC ACID RELEASE: NOYES-WHITNEY APPROACH

Change in surface concentration (C_s) and mass transfer coefficient (K) with release time Figure 8 show the fit of

experimental data to the model equation (2). On the basis of the slope obtained from this plot, it was observed that the K (a measure of boundary layer mass transfer) values did not change significantly with change in size of the nanoparticles. With change in the particle size, the

resistance offered by the surrounding boundary layer around the particles is same, therefore no significant change in mass transfer rate was observed (table 6). However, approximately 8 times increase was observed in the K values on moving from static mode to shaking mode. This is significant in itself. The shaking mode provides a well stirred condition, thereby reducing the boundary layer resistance and increased mass- transfer rate.

The experimental data also suggests that the surface concentration (C_s) changes significantly at initial time, shows a maximum and then decreases gradually with release time. It also changes significantly with cross-linking cation (figure 9). We hypothesize that there is an initial increase in surface concentration with drug release from the surface. However, as the particle size begins to decrease, the rate of dissolution decreases while transport across the boundary layer depletes the concentration next to the particle. Thus, calcium chloride cross-linked (where rate of release is higher) particles show a much higher concentration than with zinc chloride cross-linked particles. Moreover, shaking conditions leads to significant changes in surface concentration. The initial increase in C_s is due to the higher release rates recorded initially.

As the particle size is bigger, folic acid releases at higher rates. On the other hand, the mass transfer of released folic acid is slow due to which C_s increases initially. However, with increase in time, the release rates of folic acid become lower due to decrease in particle size. As the mass transfer across boundary layer is occurring at same rate, decrease in C_s was recorded.

It was observed that C_s values were significantly lower in shaking conditions than in static conditions.

Size	Cross-linking cation	Mode	K (hr ⁻¹)
500 nm	Zinc	Static	0.0006871
350 nm	Zinc	Static	0.000693
200 nm	Zinc	Static	0.0004263
500 nm	Zinc	Shaking	0.0048753
500 nm	Calcium	Static	0.00065161

This is due to higher mass transfer and reduced boundary-layer resistance.

Prediction of release behavior with the model

We use this model to predict the release behavior of different size of nanoparticles cross-linked with same cation. We have seen that the K values did not change much with the size of the nanoparticles and cross-linking cation; while, C_s values change significantly with cross-linking cation.

The predicted values calculate the concentration of folic acid in solution using the Whitney Noyes model with values of C_s from figure 9 and accounting for changing particle size with dissolution. It was observed that for a given values of K and C_s of a particular size of nanoparticle, this model can predict the release behavior of different size of nanoparticle cross-linked with same cation. Figure 10 represents the experimental concentration (C_t , experimental) and predicted concentration (C_t , predicted) of folic acid release for 250nm particle from K and C_s values of 500nm particle cross-linked with Ca²⁺.

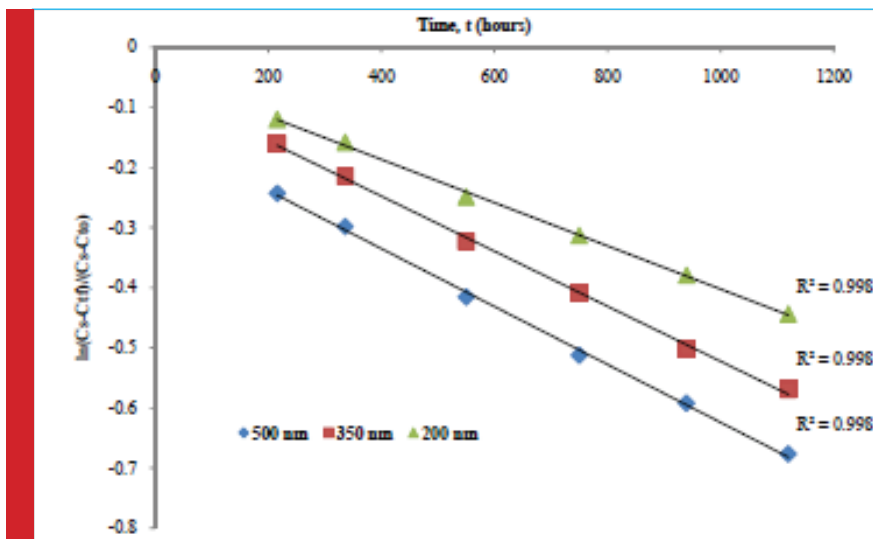


FIGURE 8: Plot of $\ln (C_s - C_t) / (C_s - C_\infty) \text{ v/s } t$ for different size of nanoparticles in static mode.

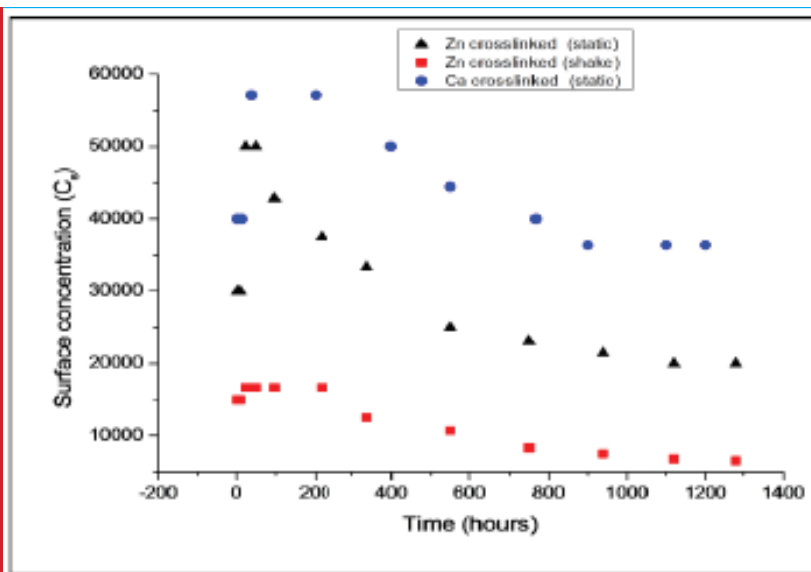


FIGURE 9: Plot of C_s ($\mu\text{g/ml}$) v/s t shows the decrease in the surface concentration from 500 nm particles with release time.

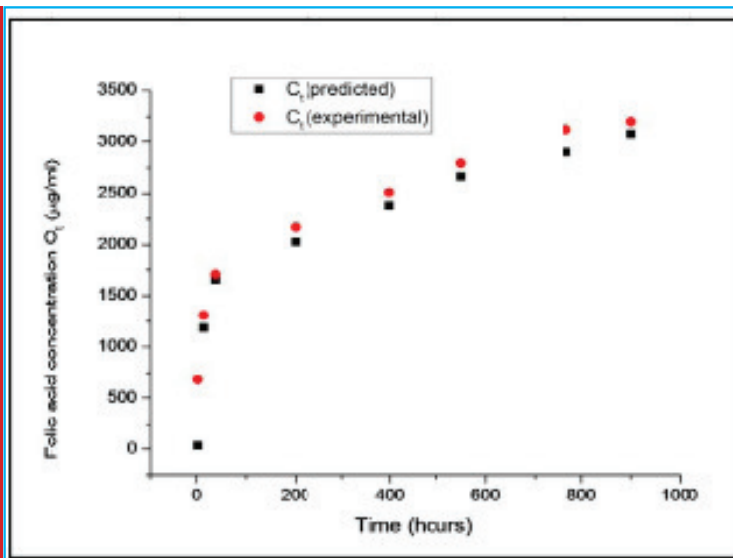


FIGURE 10: Using K & C_s values of 500 nm particle, prediction of release for 250 nm particle cross-linked with same cation (Ca^{2+}) through the model.

CONCLUSION

Folic acid release with the folate nanoparticles has been optimized with a CCD design of RSM approach. All the factors affect the response positively. A quadratic model developed accounted for all the factors considered under study. RSM approach helped in understanding the inter-

actions between any two independent factors and how these factors affect the release of folic acid from folate nanoparticles. The statistical analysis of data suggests that the model developed is significant and the predicted data was in accordance with the experimental data. This analysis provides us with an understanding of the combined effect of various process parameters

on release rates of folic acid. Moreover, the RSM model also helps to identify conditions for optimized release of folic acid. However, the model has to be re-assessed for different drugs using data sets for each drug to decide design parameters for optimal release. It gives us a heuristic understanding of how release depends on various parameters but little physical understanding.

A first order approximate drug dissolution model was developed for prediction of folic acid release and understanding the underlying mechanism. Noyes-Whitney equation was the good approximation for the release behavior. Mass transfer coefficient did not change with different size of nanoparticles significantly but increased to 8 fold in shaking conditions. It was assumed that C_s is not constant with time. This assumption was found true. C_s initially increased due to boundary layer diffusion resistance but then decreases further due to mass transfer across boundary layer. It was observed that cross-linking cation has marked effect on change in surface concentration. C_s values decreases significantly in shaking conditions due to higher mass transfer rate. Except during the initial phase, this model fairly describes the folic acid release behavior both in static and shaking mode. Moreover, at given K and C_s values for a particular size of nanoparticles, it can closely predict the release pattern of other size of nanoparticles cross-linked with same cation.

ACKNOWLEDGEMENTS

The authors would like to thank Department of Science and Technology, Government of India and Indian Institute of Technology-Delhi, India for financial support of this project.

REFERENCES

- J. Siepmann, F. Siepmann. (2013). Mathematical modeling of drug dissolution. *Int J Pharm.* 453 (1), 12–24.
- J. Siepmann, N.A. Peppas (2001). Modeling of drug release from delivery systems based on hydroxypropyl methylcellulose (HPMC), *Adv. Drug Deliv. Rev.* 48, 139–157.
- D.Y. Arifin, L.Y. Lee, C.H. Wang (2006). Mathematical modeling and simulation of drug release from microspheres: implications to drug delivery systems. *Adv. Drug Deliv. Rev.* 58, 1274–1325.
- N. Ashlee, F. Versypt, W. Daniel Pack, R. D. Braatza (2013). Mathematical Modeling of Drug Delivery from Autocatalytically Degradable PLGA Microspheres—A Review *J Control Release.* 165(1), 29–37.
- C.C. Lin, A.T. Metters (2006). Hydrogels in controlled release formulations: network design and mathematical modeling. *Adv. Drug Deliv. Rev.* 58, 1379–1408 (2006).
- B. Narasimhan (2001). Mathematical models describing polymer dissolution: consequences for drug delivery. *Adv. Drug Deliv. Rev.* 48, 195–210.
- V. Lemaire, J. Bélair, P. Hildgen (2003). Structural modeling of drug release from biodegradable porous matrices based on a combined diffusion/erosion process. *Int. J. Pharm.*, 258, 95–107.
- S. Mallapragada, N. Balaji (1998). Drug Delivery System In “Handbook of Biomaterials Evaluation: Scientific, Technical and Clinical Testing of Implant materials”. Edited by Recum, A. CRC Press, Chapter 27, 2nd edition.
- B. Narsimhan, N. Peppas (1997). Molecular Analysis of Drug Delivery Systems Controlled by Dissolution of the Polymer Carrier. *J Pharm. Sci.* 86, 297–304 (1997).
- M.S. Vaidyanathan, P. Sathyanarayana, P.K. Maiti, S.S. Visweswariah, K.G. Ayappa (2014). Lysis dynamics and membrane oligomerization pathways for Cytolysin A (ClyA) pore-forming toxin. *RSC Adv* 4, 4930–42.
- P.R. Somvanshi, K.V. Venkatesh (2013). A conceptual review on systems biology in health and diseases: from biological networks to modern therapeutics. *Syst Synth Biol*, doi 10.1007/s11693-013-9125-3.
- C. Gadgil (2008). Stochastic modeling of biological reactions. *J Ind Inst Sci*, 88, 45–55.
- P. Costo, J.M.S. Lobo (2001). Modeling and comparison of dissolution profiles. *Eur J Pharm Sci* 13,123–133.
- G. E. P. Box, K.B. Wilson (1951). On the Experimental Attainment of Optimum Conditions, *J Royal Stat Soc Ser, B*13, 1–45.
- M.A. Bezarra, R.E. Santelli, E.P. Oliveira, L.S. Villar, L.A. Escalreira (2008). Response surface methodology (RSM) as a tool for optimization in analytical chemistry. *Talanta* 76, 965–77.
- J. A. Ko, H. J. Park, Y. S. Park, S. J. Hwang, J. B. Park (2003). Chitosan microparticle preparation for controlled drug release by response surface methodology. *J Microencapsul.* 20, 791–7.
- K. Kumari, K. Prasad, P. P. Kundu (2009), Optimization of chlorpheniramine maleate (CPM) delivery by response surface methodology – four component modeling using various response times and concentrations of chitosan-alanine, glutaraldehyde and CPM. *Polymer Letters*, 3, 207–218.
- R. Misra, M. Lonare, R. Gupta, S. Mohanty (2014), Engineering folate nanoparticle nanoparticles through liquid-crystalline folate solutions. *Sci. Adv. Mater.* 6, 835–843.
- R. Misra, H. Katyal, S. Mohanty (2014). Controlled release of folic acid through liquid-crystalline folate nanoparticles, *Mat Sci & Eng C* 44, 352–361.
- R. Misra, S. Mohanty (2014). Sustained release of methotrexate through liquid-crystalline folate nanoparticles. *J Mater Sci: Mater Med.* DOI 10.1007/s10856-014-5257-6.
- R.H. Myers (1976). *Response Surface Methodology*, Boston: Allyn and Bacon.
- S.G. Gilmour (2006). Response surface designs for experiments in bioprocessing. *Biometrics* 62, 323–331.
- S. Chowdhury, P.D. Saha (2012). Scale-up of a dye adsorption process using chemically modified rice husk: optimization using response surface methodology. *Deswater* 37, 331–336.